Accretion disc-corona models and X/γ-ray spectra of accreting black holes

By JURI POUTANEN

Stockholm Observatory, SE - 133 36 Saltsjöbaden, Sweden

We discuss properties of thermal and hybrid (thermal/non-thermal) electron-positron plasmas in the pair and energy equilibria. Various accretion disc-corona models, recently proposed to explain properties of galactic as well as extragalactic accreting black holes, are confronted with the observed broad-band X-ray and γ-ray spectra.

1. Introduction

It was realized quite early that broad-band X/γ-ray spectra of Galactic black holes (GBHs) can be explained in terms of successive Compton scatterings of soft photons (Comptonization) in a hot electron cloud. The Comptonizing medium was assumed to be thermal with a given temperature, T_e, and a Thomson optical depth, τ_T. The theoretical spectra were computed by analytical (Shapiro, Lightman & Eardley 1976; Sunyaev & Titarchuk 1980) and Monte-Carlo methods (Pozdnyakov, Sobol' & Sunyaev 1983).

The problem with such an approach is that in any specific geometry arbitrary combinations of (τ_T, T_e) are not possible. Both GBHs and Seyfert galaxies show a hardening of the spectra at ~ 10 keV, which is attributed to Compton reflection (combined effect of photo-electric absorption and Compton down-scattering) of hard radiation from a cold material (White, Lightman & Zdziarski 1988; George & Fabian 1991). Hard radiation, reprocessed in the cold matter, can form a significant fraction of the soft seed photons for Comptonization. The energy balance of the cold and hot phases determine their temperatures and the shape of the emerging spectrum (Haardt & Maraschi 1991, 1993; Stern *et al.* 1995b; Poutanen & Svensson 1996).

The situation becomes more complicated when a notable fraction of the total luminosity escape at energies above ~ 500 keV. Then hard photons can produce $e^{\pm}$ pairs which will be added to the background plasma. Electrons (and pairs) Comptonize soft photons up to γ-rays and produce even more pairs. Thus, the radiation field, in this case, has an influence on the optical depth of the plasmas, which in its turn produces this radiation. This makes the problem very non-linear.

Another complication appears when the energy distribution of particles starts to deviate from a Maxwellian. In the so called non-thermal models, relativistic electrons are injected to the soft radiation field. The steady-state electron distribution should be computed self-consistently, balancing electron cooling (e.g., by Compton scattering and Coulomb interactions) and acceleration, together with the photon distribution. The pioneering steps in solving this problem were done by Stern (1985, 1988) using Monte-Carlo techniques and by Fabian *et al.* (1986), Lightman & Zdziarski (1987), Coppi (1992) using the method of kinetic equations (see Stern *et al.* 1995a; Pilla & Shaham 1997; Nayakshin & Melia 1998, for recent developments). Non-thermal model have been used extensively in the end of 1980s and beginning of 1990s for explaining the X-ray spectra of active galactic nuclei (see, e.g., Zdziarski *et al.* 1990), while recently pure thermal model were preferred, since the data show spectral cutoffs at ~ 100 keV in both GBHs and Seyferts (Grebenev *et al.* 1993, 1997; Johnson *et al.* 1997). However, power-law like

spectra extending without a cutoff up to at least ~ 600 keV, observed in some GBHs in their soft state (Grove *et al.* 1997a,b), give new strength to the undeservedly forgotten non-thermal models.

Spectral fitting with multi-component models following simultaneously energy balance and electron-positron pair balance, give stronger constraints on the physical condition in the X/γ-ray source, its size and geometry, presence of $e^{\pm}$ pairs, and give a possibility to discriminate between various accretion disc models. In this review, we first describe thermal as well as non-thermal pair models that have been used recently for spectral fitting of GBHs and Seyferts. We discuss spectral properties of $e^{\pm}$ plasmas in energy and pair equilibria for various geometries of the accretion flow. Separately for GBHs and Seyferts, we briefly review X/γ-ray observations. Then, we consider physical processes responsible for spectral formation and confront phenomenological models of the accretion discs with data. We restrict our analysis to "radiative" models where radiative processes and radiative transfer in realistic geometries are considered in details while heating and acceleration mechanisms are not specified.

2. Spectral models

2.1. *Thermal (pair) plasmas*

Since spectra of both Seyferts and GBHs in their hard states cutoff sharply at ~ 100 keV (Grebenev *et al.* 1993, 1997; Zdziarski *et al.* 1996a,b, 1997; Grove *et al.* 1997a,b), thermal models are in some preference.

2.1.1. *General properties*

First, we consider properties of an electron (-positron) plasma cloud in energy and pair equilibria without assuming any specific geometry of the accretion flow. There are four parameters that describe the properties of hot thermal plasmas: (i) $l_h \equiv L_h\sigma_T/(m_ec^3r_c)$, the hard compactness which is the dimensionless cloud heating rate; (ii) the soft photon compactness, l_s, which represents the cold disc luminosity that enters the hot cloud (corona); (iii) τ_p, the proton (Thomson) optical depth of the cloud (i.e.., the optical depth due to the background electrons); and (iv) the characteristic temperature of the soft photons, $T_{\rm bb}$. Here r_c is the cloud size, σ_T is the Thomson scattering cross-section. In this simplified description, energy and pair balance equations have been solved using analytical and numerical methods (Zdziarski 1985; Ghisellini & Haardt 1994; Pietrini & Krolik 1995; Coppi 1992; Stern *et al.* 1995a).

For sufficiently high compactnesses, the total optical depth can be significantly larger than τ_p. In that case, increase in the cloud heating rate results in the corresponding increase of the cloud total optical depth, τ_T, due to $e^{\pm}$ pairs produced, and in decrease of the cloud temperature, T_e. The ratio l_h/l_s (the amplification factor) has a one-to-one correspondence with the Kompaneets y-parameter (e.g., Rybicki & Lightman 1979), which can be related to the spectral index of the emitted spectrum (see Fig. 1). The spectral index stays approximately constant for a constant Kompaneets y-parameter ($y = 4\Theta\tau_T$, for parameters of interest, here $\Theta \equiv kT_e/m_ec^2$).

Pietrini & Krolik (1995) proposed a very simple analytical formula that relates the observed X-ray spectral energy index to the amplification factor:

$$\alpha \approx 1.6 \left(\frac{l_h}{l_s}\right)^{-1/4}. \qquad (2.1)$$

Though the exact coefficient of proportionality depends on the electron temperature and

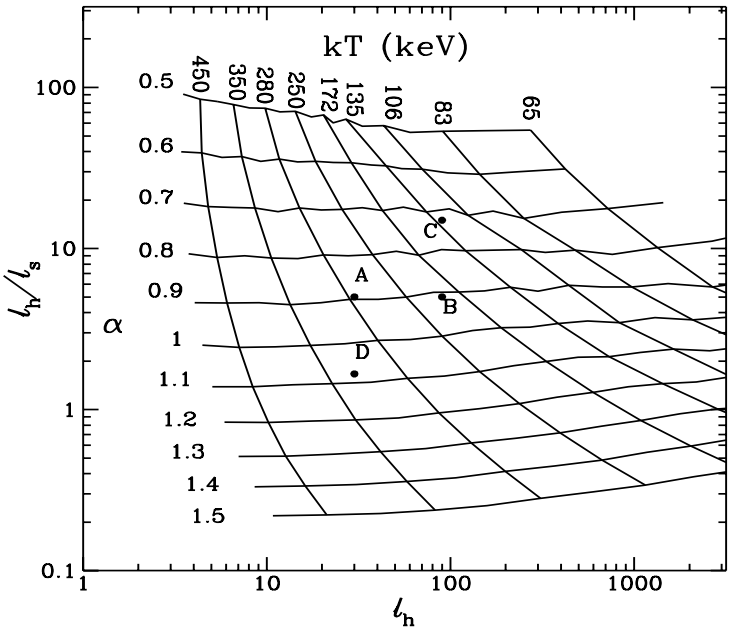

FIGURE 1. Mapping of $(l_h, l_h/l_s)$ to (α, T_e) (from Ghisellini & Haardt 1994). The compactnesses are defined as follows: $l_{h,s} \equiv L_{h,s}\sigma_T/(m_e c^3 r_c)$, where r_c is the size of the hot cloud, L_h is the heating rate of the hot cloud, and L_s is the luminosity of the seed soft photons that cool the plasma. This relation holds for $e^{\pm}$ pairs dominated plasmas. For electron-proton dominated plasmas, (α, T_e) depend on $(\tau_T, l_h/l_s)$. One sees that ratio l_h/l_s almost uniquely defines the spectral energy index, α.

the energy of seed photons, this dependence is rather weak. When l_h/l_s increases (the source becomes more "photon starved"), the observed spectrum becomes harder.

2.1.2. *Geometry*

We consider here various geometrical arrangements of the hot plasma cloud and the source of soft photons (see Haardt 1997 for a recent review). The observed spectra of GBHs and Seyferts correspond to $y \approx 1$. This fact does not have a direct explanation in the accretion disc framework. If soft seed photons for Comptonization are produced by reprocessing hard X/γ-ray radiation, then the geometry will define the amplitude of feedback effect and the spectral slope (Liang 1979). What would be the most probable geometry?

Sandwich. The simplest solution is to assume that a hot corona covers most of the cold disc (a sandwich, or a slab-corona model). The radiative transfer in such a geometry was considered by Haardt & Maraschi (1991, 1993) who showed that in the extreme case, when all the energy is dissipated in the corona, the emitted spectra resemble those observed in Seyfert galaxies. Dissipation of energy in the cold disc (with subsequent additional production of soft photons) would produce too steep spectra in disagreement with observations. Even harder spectra observed in GBHs cannot be reconciled with the slab-corona model (Dove *et al.* 1997; Gierliński *et al.* 1997a; Poutanen, Krolik & Ryde 1997), and alternative models with more photon starved conditions and smaller feedback of soft photons are sought.

Magnetic flares. A patchy corona (Galeev, Rosner & Vaiana 1979; Haardt, Maraschi & Ghisellini 1994), where the cold disk is not covered completely by hot material, has certainly a smaller feedback, and the resulting spectra are harder. A patchy corona can be described by a number of active regions above the cold accretion disc. Spectral properties of an active region in the energy and pair balance have been computed recently by Stern *et al.* (1995b) (see also reviews by Svensson 1996a,b for more details). Both patchy and slab-corona models predict an *anisotropy break* (i.e. a break in the power-law spectrum due to the anisotropy of the seed photons) that should appear at the energy corresponding to the second scattering order.

Cloudlets. Another possible solution of the photon starvation problem is to assume that the cold disc within the hot corona is disrupted into cold dense optically thick clouds (Lightman 1974; Celotti, Fabian & Rees 1992; Collin-Souffrin *et al.* 1996; Kuncic, Celotti & Rees 1997) that are able to reprocess hard X/γ-ray radiation and produce soft seed photons for Comptonization. If the height-to-radius ratio of the hot cloud is small, we can approximate this geometry by a plane-parallel slab. We assume further that the cold material is concentrated in the central plane of the hot slab and has a covering factor f_c. Compton reflection comes from these cold clouds (cloudlets) as well as from the outer cooler disc. The seed soft photon radiation is much more isotropic and the emerging high energy spectrum does not have an anisotropy break. The covering factor defines the amplitude of the feedback effect. The total soft seed luminosity (with corresponding compactness, l_s) is the sum of the reprocessed luminosity and the luminosity intrinsically dissipated in the cold disc (with corresponding compactness, $l_s^{\rm intr}$). For a slab geometry, the heating rate, L_h, of a cubic volume of size h determines the hard compactnesses $l_h \equiv L_h\sigma_T/(m_ec^3h)$ (where h is the half-height of the slab). Other compactnesses are defined is a similar way.

Figure 2 shows the dependence of the electron temperature and the optical depth on parameters of the cloudlets model, and Figure 3 gives a few selected spectra. Using the method of Poutanen & Svensson (1996), we solve the energy and pair balance equations coupled with the radiative transfer accounting for Compton scattering (exact redistribution function is employed, see, e.g., Nagirner & Poutanen 1994), pair production and annihilation, and Compton reflection. We should point out that in the case of pair dominated plasmas, increase in the amount of soft photons does not necessarily imply a decrease in the plasma temperature. The optical depth decreases rapidly with increase of $l_s^{\rm intr}/l_h$, and the average energy available per particle can even increase. In the case of electron-proton plasmas, $\tau_T \approx \tau_p$ and T_e decreases with increasing internal dissipation in the cold disc.

"Sombrero". In this model, the cold disc penetrates only a short way into the central coronal region (see, e.g., Bisnovatyi-Kogan & Blinnikov 1977, and Poutanen *et al.* 1997 for recent applications). We can assume that the X/γ-ray source can be approximated by a homogeneous spherical cloud of radius r_c situated around a black hole (probably, a torus geometry for a hot cloud would be more physically realistic, but then it would be more difficult to compute the radiative transfer). The inner radius, r_{in}, of the cold geometrically thin, infinite disc is within the corona ($r_{in}/r_c \leq 1$). This geometry is also similar to the geometry of the popular advection dominated accretion flows (see article by R. Narayan, R. Mahadevan, and E. Quataert in this volume). Spectra from the sombrero models are almost identical to the spectra expected from the cloudlets model, with the only difference that the amount of Compton reflection would be a bit larger for the same configuration of the outer cooler disc. From the observational point of view, these models are almost indistinguishable.

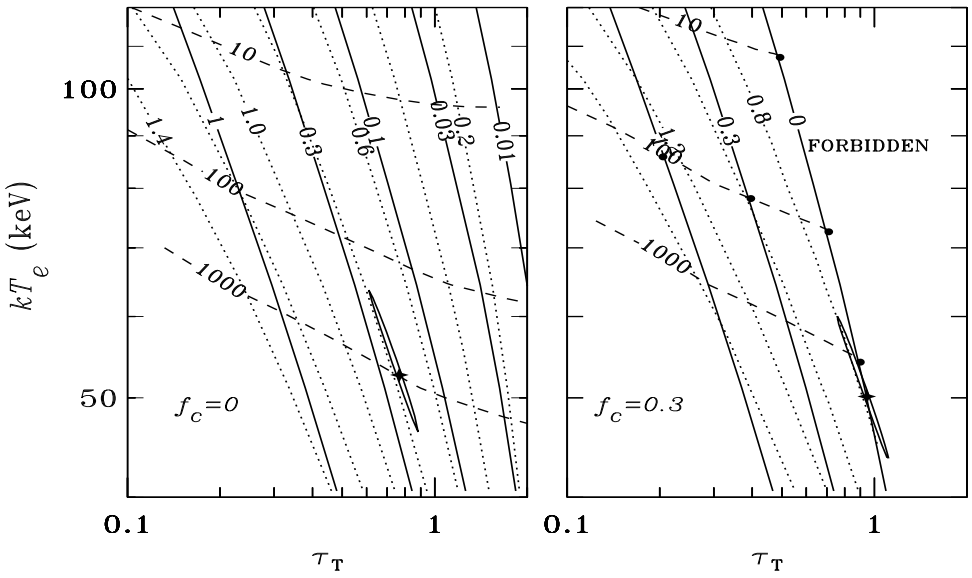

FIGURE 2. Relation between total optical depth, τ_T, of the half-slab and electron temperature, kT_e, for the cloudlets model. Here cold matter is assumed to be concentrated in the central plane of the hot slab. Temperature of cloudlets is fixed at $kT_{\rm bb} = 0.25$ keV. The covering fraction of the cold material is taken to be $f_c = 0$ (left panel) and $f_c = 0.3$ (right panel). For $f_c = 0$, all seed photons are external. Solid curves represent solutions for constant $l_s^{\rm intr}/l_h$. These relations are the same for pure pair or pure electron-proton plasmas. The dashed curves are the solutions for a constant l_h (assuming pair dominated plasmas, i.e., $\tau_p \ll \tau_T$, and thermal electron distribution). Dotted curves give solutions for a constant intrinsic (without Compton reflection) spectral index α in 2–18 keV range. $l_s^{\rm intr}$ can mean here both intrinsic internally (not reprocessed) and externally produced soft photon luminosity. Region to the right of $l_s^{\rm intr}/l_h = 0$ curve is forbidden (the energy balance cannot be reached). Stars represent best fits to the simultaneous *Ginga* and OSSE data of GX 339-4 in September 1991 (Zdziarski *et al.* 1998) and elongated ellipsoids are the contours plots at 90 per cent confidence level for two interesting parameters ($\Delta\chi^2 = 4.61$). For GX 339-4, external or internally produced soft luminosity (not reprocessed) entering hot slab can be $\sim 23\%$ of the heating rate L_h, if $f_c = 0$. If $f_c = 0.3$, the only solution describing data of GX 339-4 is possible when there are *no* internally generated (except reprocessed) or external soft photons. Cooling is provided by reprocessed radiation only. Spectra for the solutions marked by filled circles are shown in Figure 3.

2.2. *Hybrid thermal/non-thermal pair plasmas*

There are reasons to believe that in a physically realistic situation, the electron distribution can notably deviate from a Maxwellian. A significant fraction of the total energy input can be injected to the system in form of relativistic electrons (pairs). In the so called hybrid thermal/non-thermal model, the injection of relativistic electrons is allowed in addition to the direct heating of thermal electrons.

The most important input parameters of the model are: (i) the thermal compactness, l_{th}, which characterizes the heating rate of electrons (pairs); (ii) the analogous non-thermal compactness, l_{nth}, which characterizes the rate of injection of relativistic electrons, (iii) the soft photon compactness, l_s; (iv) Γ_{inj}, the power-law index of the non-thermal electron injection spectrum, (v) τ_p, the proton (Thomson) optical depth; and (vi) T_{bb}. Compton reflection adds a few more parameters (e.g. the amplitude R, the ionisation parameter ξ) and can be accounted for using angular dependent Green's functions (Magdziarz & Zdziarski 1995; Poutanen, Nagendra & Svensson 1996). By

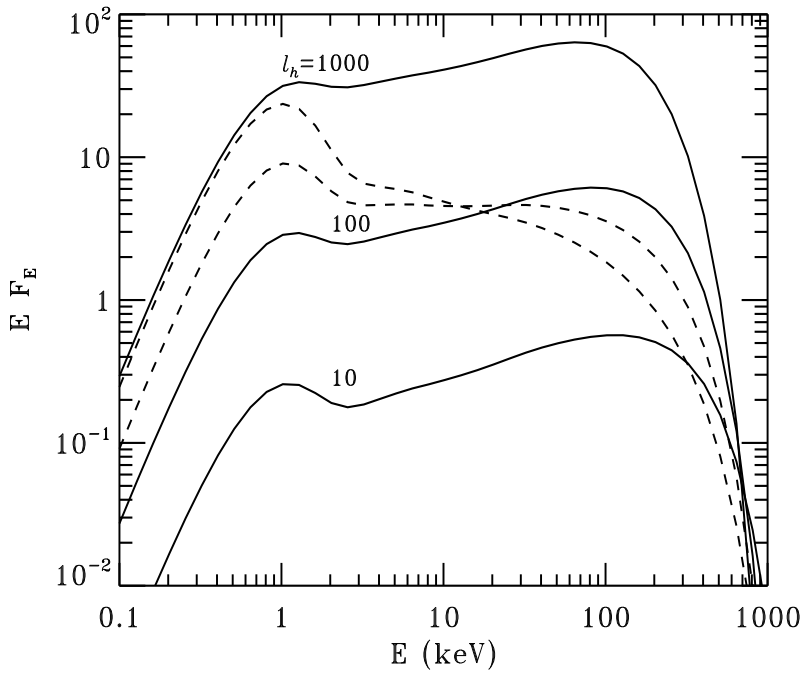

FIGURE 3. Spectra from the hot slab - cold clouds model for solutions represented by filled circles in Figure 2. Solid curves correspond to the solutions with no internal dissipation in the cold clouds ($l_s^{\rm intr}=0$) and various hard compactness l_h. Dotted curves correspond to $l_h=100$, and $l_s^{\rm intr}/l_h=0.3$ and 1. With increasing $l_s^{\rm intr}/l_h$ spectra become steeper (softer), but the electron temperature does not decrease (rather slowly increases). In the case of the electron-proton plasmas, T_e would decrease rapidly with constant $\tau_T\approx\tau_p$.

$l_h=l_{th}+l_{nth}$, we denote the total hard compactness. For spectral fitting, we use the code of Coppi (1992) (see also Coppi *et al.* 1998) which is incorporated into the standard X-ray data analysis software XSPEC.

The electron distribution is computed self-consistently balancing electron cooling (by Compton scattering and Coulomb interactions), heating (thermal energy source), and acceleration (non-thermal energy source). The self-consistent electron (-positron) distribution can be characterized by a Maxwellian of the equilibrium temperature, T_c, plus a non-thermal (generally not a power-law) tail. The spectrum of escaping radiation then consists of the incident blackbody, the soft excess due to Comptonization by a *thermal* population of electrons and a power-law like tail due to Comptonization by a *non-thermal* electron (pair) population.

As a first example, we consider how spectra from the hybrid plasmas change with the hard compactness when keeping the ratio of the soft-to-hard compactness constant (this gives an almost constant α) and fixing the non-thermal efficiency (l_{nth}/l_h) at 10 per cent (see solid curves in Figure 4). The electron temperature behaves exactly as in the pure thermal case (it decreases when compactness increases), since relatively small non-thermal efficiency, that we have chosen, does not change the energy balance significantly. The electron distribution is Maxwellian with a weak high energy tail.

Next, we consider how the spectra change as a function of l_h/l_s, while keeping the other parameters constant. The dashed curves in Figure 4 show the evolution of the spectrum with increasing soft seed photon luminosity. For large l_h/l_s, most of the spectrum is

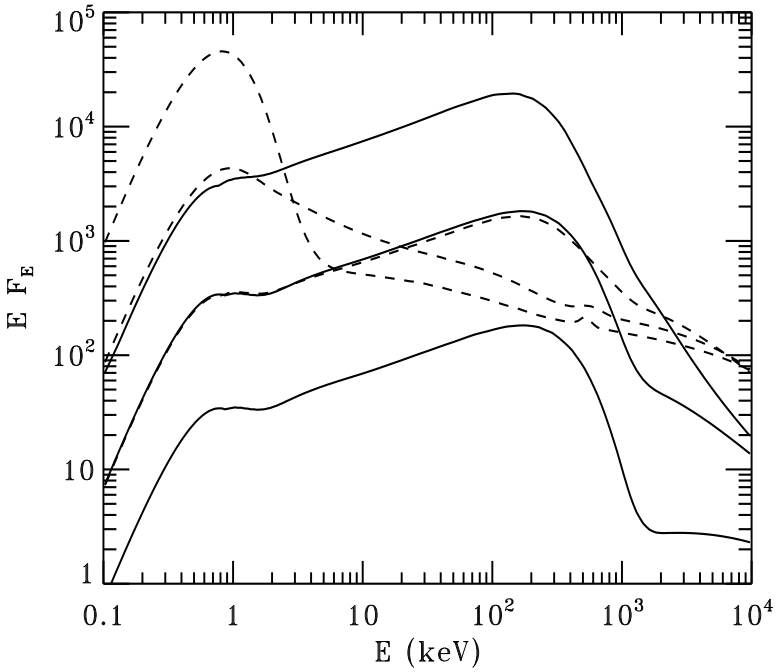

FIGURE 4. Spectra from the hybrid pair plasmas. Solid curves show dependence on hard compactness l_h. Other parameters: $l_h/l_s = 10$, $l_{nth}/l_h = 0.1$, $\tau_p = 1$, $\Gamma_{inj} = 2.5$, $T_{\rm bb} = 0.2$ keV. The resulting electron temperature and optical depth are (kT_e, τ_T)=(126 keV, 1.0002), (123 keV, 1.02), and (82 keV, 1.47) for $l_h = 1, 10, 100$, respectively (l_h increases from the bottom to the top of the figure). For a higher compactness, the spectrum has a sharper cutoff at energies above 1 MeV due to larger optical depth for photon-photon pair production. These spectra are similar to the spectra of GBHs in their hard state (see Fig. 5). Dashed curves show dependence on l_h/l_s. Here we fixed $l_h = 10$, $l_{nth}/l_h = 0.5$. The resulting electron temperature and optical depth (kT_e, τ_T) are (104 keV, 1.07), (34 keV, 1.02), and (5 keV, 1.01) for $l_h/l_s = 10, 1, 0.1$, respectively. Increase in l_s results in a more pronounced blackbody part of the emerging spectrum. The blackbody is modified by Comptonization on thermal electrons.

produced by Comptonization off a *thermal* population of electrons (pairs), while the tail at energies above $m_e c^2$ is produced by *non-thermal* electrons. For low l_h/l_s, the electron temperature drops. Most of the pairs are in the thermal bump, but Kompaneets y-parameter is very small since the electron temperature is small. The resulting spectrum is produced by a *single* Compton scattering off non-thermal electrons. The Maxwellian part of the electron distribution produces a weak power-law tail to the blackbody bump. The annihilation line is quite weak for relatively small compactnesses, and would not be detectable by modern detectors. The cutoff energy at a few MeV is anti-correlated with the compactness.

Quantitatively, the behaviour of the electron distribution with changing of the amount of soft photons is easy to understand. A break between thermal and non-thermal parts of the electron distribution appears where the thermalization timescale due to Coulomb scattering is equal to the Compton cooling timescale (we neglect here thermalization by synchrotron self-absorption, see, e.g., Ghisellini & Svensson 1990; Ghisellini, Haardt, & Svensson 1998). Compton cooling timescale is simply $t_{Compton} = \pi r_c/(\gamma c l_s)$, while Coulomb thermalization operates at $t_{Coulomb} \approx \gamma r_c/(\tau_T c \ln\Lambda)$ timescale (see, e.g., Dermer & Liang 1989; Coppi 1992; Ghisellini, Haardt, & Fabian 1993; here $\ln\Lambda$ is the usual

Coulomb logarithm, typically ~ 15, and γ is the electron Lorentz factor). These relations define the Lorentz factor of the break

$$\gamma_{break} \approx \left(\pi \ln\Lambda \frac{\tau_T}{l_s}\right)^{1/2}. \tag{2.2}$$

Increase in Compton cooling causes the break to shift towards lower energies.

3. Galactic black holes

3.1. *Hard state of Galactic black holes*

3.1.1. *Observations and interpretation*

Galactic black holes (GBHs) are observed in a few different spectral states that can be generally classified as soft and hard. A spectrum in the hard state is characterized by a power-law with the energy spectral index $\alpha \approx 0.4-0.9$ with a cutoff at energies $\sim$ 100 keV (Grebenev *et al.* 1993, 1997; Tanaka & Lewin 1995; Phlips *et al.* 1996; Zdziarski *et al.* 1996a, 1997; Grove *et al.* 1997a,b). The presence of an iron line at ~ 6.4 keV and an iron edge at ~ 7 keV, together with a spectral hardening around 10 keV, was interpreted as a signature of Compton reflection of the intrinsic spectrum from relatively cold matter (Done *et al.* 1992; Ebisawa *et al.* 1996b; Gierliński *et al.* 1997a). The amount of Compton reflection $R \equiv \Omega/2\pi \approx 0.3-0.5$ ($R=1$ corresponds to an isotropic X/γ-ray source atop an infinite cold slab). An excess at energies $\lesssim 1$ keV is interpreted as radiation from the accretion disc (Bałucińska & Hasinger 1991; Bałucińska-Church *et al.* 1995) with a characteristic temperature, $T_{\rm bb}$, of order 0.1 – 0.3 keV (usually quite poorly determined, due to strong interstellar absorption in that spectral range). Observations by BATSE and COMPTEL revealed also a presence of a high energy excess at $\gtrsim 500$ keV in some GBHs (Cyg X-1: McConnell *et al.* 1994; Ling *et al.* 1997; GRO J0422+32: van Dijk *et al.* 1995). The monochromatic luminosity, EL_E, peaks at about ~ 100 keV. A characteristic spectrum of the hard state GBH is shown in Figure 5.

GBHs show variability in X/γ-rays on all possible time scales, from milliseconds to years. The size of the emitting region cannot be much larger than the minimum variability time scale $\times c \approx 1$ ms $\times c = 300$ km. In the context of accretion onto a black hole it is 10 gravitational radii, $R_g \equiv GM/c^2$, (for a 10 $M_\odot$ black hole), i.e., the inner part of the accretion disc where most of the energy is liberated. Since, in the hard state, GBHs radiate a big fraction of the energy in the hard X-rays/soft γ-rays (see Figs. 5, 8), the region responsible for the production of this radiation lies within $\sim 20-50R_g$. The most efficient cooling mechanism responsible for formation of the spectra is probably thermal Comptonization of soft photons in the $\sim 50-100$ keV electron cloud and $\tau_T \sim 1$ (Shapiro *et al.* 1976; Zdziarski *et al.* 1996a, 1997; Gierliński *et al.* 1997a). High sensitivity OSSE observations in the 50-500 keV range allow to determine the electron temperature to within 10 per cent. High energy ($\gtrsim 300$ keV) excesses can be explained only if one introduces an additional spectral component. This component can be produced either in a spatially separated, much hotter region by thermal Comptonization (Liang & Dermer 1988; Liang 1991; Ling *et al.* 1997), or in the same region by a non-thermal tail of the electron distribution (Li, Kusunose & Liang 1996a,b; Poutanen & Coppi 1998). In the former (thermal) case, the very hot ~ 400 keV plasma cloud has to be kept far from the sources of soft photons to avoid cooling, and it is not clear whether one can physically separate it from the rest of the accretion disc. Having a very hot cloud close to the ~ 100 keV inner disc, could also be a problem since radiative conduction would smooth out large temperature gradients. On the other hand, non-thermal tails can be created by

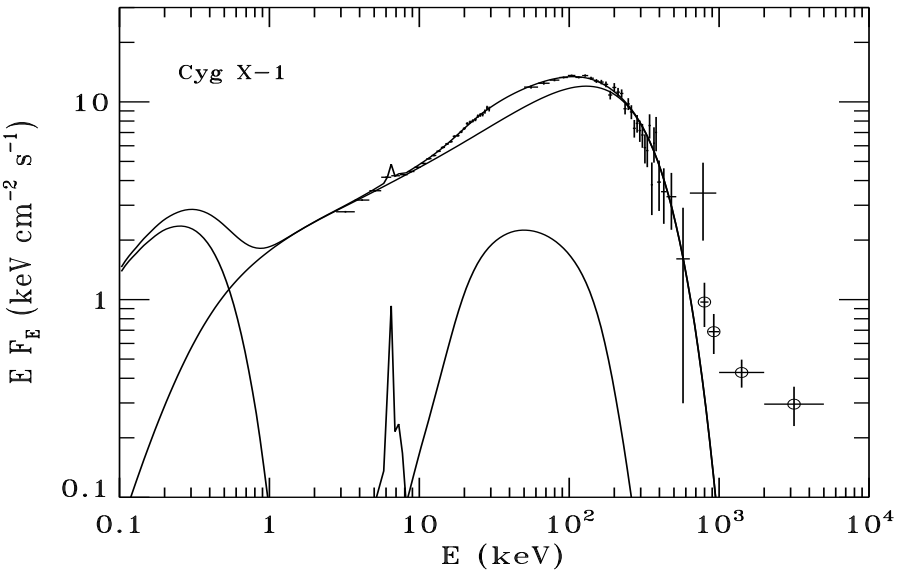

FIGURE 5. The hard state of Cygnus X-1. Simultaneous *Ginga*, OSSE and COMPTEL data from June 1991. Different components correspond to the soft blackbody radiation, thermal Comptonized spectrum, and its Compton reflection. A high energy excess at $\gtrsim 1$ MeV cannot be described by thermal models.

magnetic processes which likely operate in the accretion disc environment (see Dermer, Miller & Li 1996; Li *et al.* 1996a; Li & Miller 1997 and references therein).

3.1.2. *Geometry*

Observations of the Compton reflection feature, together with a fluorescent iron line, suggest the presence of a rather cold weakly ionized material in the vicinity of the X/γ-ray source. From the amplitude of Compton reflection one can derive that the cold matter occupies $\Omega/2\pi \sim 1/3$ solid angle as viewed from the hard photon source (Ebisawa *et al.* 1996b; Gierliński *et al.* 1997a; Życki, Done & Smith 1997a). Further constraints on the geometry, e.g., the covering fraction of the hot cloud as viewed from the soft photon source, can be derived from the observed spectral slopes if the *observed* soft luminosity can be reliably estimated (Poutanen *et al.* 1997). There are no evidence that the cold material extends close to the black hole. (The observed iron lines are quite narrow, and the iron edges are quite sharp implying weakness of gravitational and Doppler effects.)

Sandwich. As we pointed out in Section 2.1.2, an accurate treatment of the radiative transfer and Compton scattering rule out slab-corona (sandwich) models for sources with hard spectra (see Poutanen *et al.* 1997; Dove *et al.* 1997 where the case of Cyg X-1 is considered, and Zdziarski *et al.* 1998 for the interpretation of GX 339-4 data). Even if all the energy is dissipated in the corona, the predicted spectra are too steep and cannot be reconciled with observations. Energy dissipation in the cold disc and the corresponding increase of the amount of seed soft photons worsen the discrepancy. The anisotropy break expected at a few keV in the sandwich model was never observed.

Flares. Magnetic flares (active regions) on the surface of the cold accretion disc also predict anisotropy break in disagreement with observations. Active regions atop the cold disc give the right amount of Compton reflection (since at $\tau_T \sim 1$, a big fraction of it is scattered away), but produce too steep spectra as in the case of the sandwich model.

Detached active regions (Svensson 1996a,b) produce spectra with the right spectral slopes while predicting too much reflection ($R \sim 1$).

Cloudlets. Zdziarski *et al.* (1998) found this model giving the best description of *Ginga* and OSSE data of GX 339-4. In this case, most of the Compton reflection occurs in an outer cold disc. The covering factor of cold clouds within the hot inner disc cannot be larger than $f_c \sim 0.3$ due to the energy balance requirements (see Fig. 2).

Sombrero. This geometry is consistent with the amount of Compton reflection observed in GBHs in their hard state (Dove *et al.* 1997; Gierliński *et al.* 1997a; Poutanen *et al.* 1997). In the case of Cyg X-1, a solution with $r_{in}/r_c = 1$ is energetically possible, but the intrinsic soft luminosity should be rather large in order to produce enough soft photons for Comptonization. The energy balance constrains the inner radius of the cold disc to be larger than $\sim 0.7 r_c$. Probably, $r_{in}/r_c = 0.8 - 0.9$ would satisfy all the observational requirements (see Poutanen *et al.* 1997). Similarly, in case of GX 339-4 (which has a steeper spectrum in the hard state than Cyg X-1), $r_{in}/r_c \geq 0.7$ required.

Concluding, models with the central hot cloud surrounded by a cold disc give the best description of the data.

3.1.3. *Spectral variability and $e^{\pm}$ pairs*

As it was already mentioned, Galactic black holes show variability on different times scale (see recent review by Van der Klis 1995). Here we just consider spectral variations on the time scales of hours. It was shown by Gierliński *et al.* (1997a) that the spectral shape of Cyg X-1 in the *Ginga* spectral range does not vary much when luminosity changes within a factor of two (Fig. 6), while there is evidence that the cutoff energy increases when luminosity drops (best fit curves cross each other at ~ 500 keV). Such a behaviour implies almost a constant ratio l_s/l_h (see Figs. 1 and 2) and a constant Kompaneets y-parameter. We can conclude that the transition radius between the hot and the cold discs does not change much (otherwise, the ratio of the intrinsic energy dissipation in the cold disc to the heating rate of the hot cloud would change, causing spectral slope changes). Alternatively, the transition radius is sufficiently large that most of the seed soft photons are provided by reprocessing hard radiation from the central cloud.

For $e^{\pm}$ pair dominated plasmas, variation in the heating rate would cause variations in the optical depth by pair production and corresponding changes of the cloud temperature. On the other hand, the same behaviour is expected when no pairs are present. Now, variations in the accretion rate cause variation in optical depth and escaping luminosity, and the temperature adjusts to satisfy the energy balance.

It is probably not possible to determine the pair content directly from observations, since spectra from the *thermal* $e^{\pm}$ plasma are indistinguishable from spectra of the electron-proton plasma (annihilation line is much too weak to be observed, see Maciołek-Niedźwiecki, Zdziarski & Coppi 1995; Stern *et al.* 1995b). It is in principle possible to determine the compactness parameter from observations. For example, in the case of Cyg X-1, $l_h \sim 20$ assuming a unitary (i.e. not broken into many pieces) source, while $l_h \sim 400$ is required to make the source pair dominated (Poutanen *et al.* 1997). If the energy dissipation is extremely inhomogeneous (which would be the case if magnetic reconnection is responsible for the energy dissipation), then at a given moment most of the luminosity is produced by a smaller fraction of the cloud and the effective compactness can be much higher. Presence of non-thermal particles in the source would increase pair production and explain the high energy excess at ~ 1 MeV at the same time. However, the quality of the data is not sufficient to make any definite conclusions.

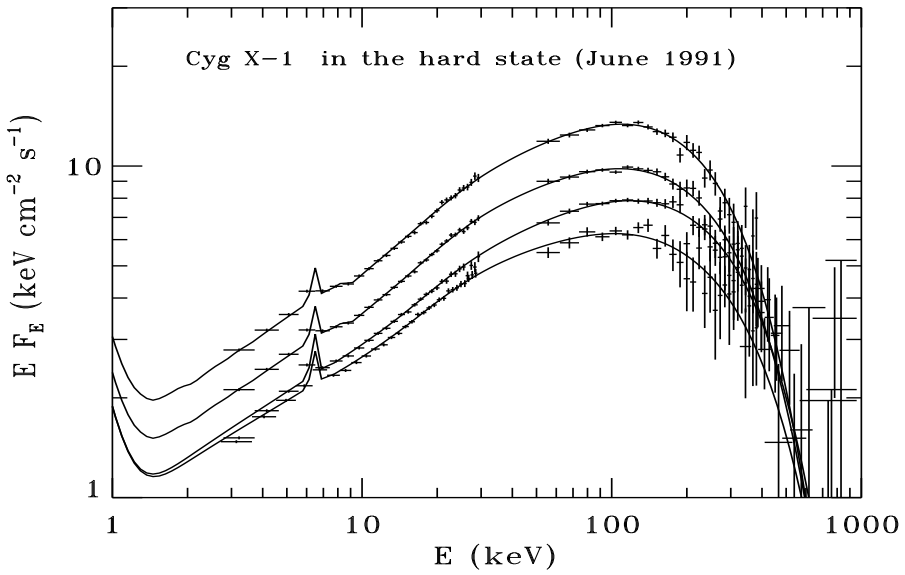

FIGURE 6. Spectral variation of Cyg X-1 on the time scales of hours in the hard state as observed by *Ginga* and OSSE in June 1991 (data are adapted from Gierliński *et al.* 1997a).

3.2. *Soft state of Galactic black holes*

3.2.1. *Observations and interpretation*

Unlike in the hard state, most of the luminosity in the soft state is carried by a blackbody like component with a characteristic temperature, $kT_{\rm bb} \approx 0.5 - 1$ keV. Until recently, there were not so many broad-band data with high spectral resolution and high signal-to-noise ratio (see, e.g., Tanaka & Lewin 1995; Grebenev *et al.* 1993, 1997) that a detailed spectral analysis would be possible. Having *ASCA, RXTE*, and *CGRO* in orbit at the same time changes the situation. Cygnus X-1 was observed by all these observatories simultaneously on May 30, 1996 and by *RXTE* and *CGRO* on June 17-18, 1996, when it was in the soft state. Figure 7 gives an example of the soft state spectrum.

A soft component (energies less than $\sim$ 5 keV) cannot be represented neither by a multicolor disc spectrum, nor a modified blackbody. It is clear that at least two component are required to fit it (e.g., blackbody and a power-law, or two black bodies, Cui *et al.* 1997a,b; Gierliński *et al.* 1997b). One can imagine that the soft blackbody comes from the accretion disc, but the nature of the additional component peaking at $\sim$ 3 keV is not so clear. Gierliński *et al.* (1997b) interpreted it as due to thermal Comptonization of a disc blackbody in a plasma with $kT_e \approx 5$ keV and $\tau_T \approx 3$.

GBH spectra in the hard X-rays/soft γ-rays can be well represented by a power-law which does not have an observable break, at least, up to energies of order $m_e c^2$ (Phlips *et al.* 1996; Grove *et al.* 1997a,b, 1998). COMPTEL has detected Cyg X-1 and GRO J1655-40 at energies up to $\sim$ 10 MeV (A. Iyudin, private communications), and it seems that the power-law at MeV energies is just a continuation of the hard X-ray power-law. Although signatures of Compton reflection are also observed in this state (e.g. Tanaka 1991), its amplitude, R, is much more difficult to determine since it depends on the assumed distribution of ionisation and detailed modelling of the continuum, which is rather curved in the spectral region around the iron edge (see Fig. 7). For example, Gierliński *et al.* (1997b) give $R \approx 0.6 - 0.8$ for Cyg X-1 in the soft state observed on

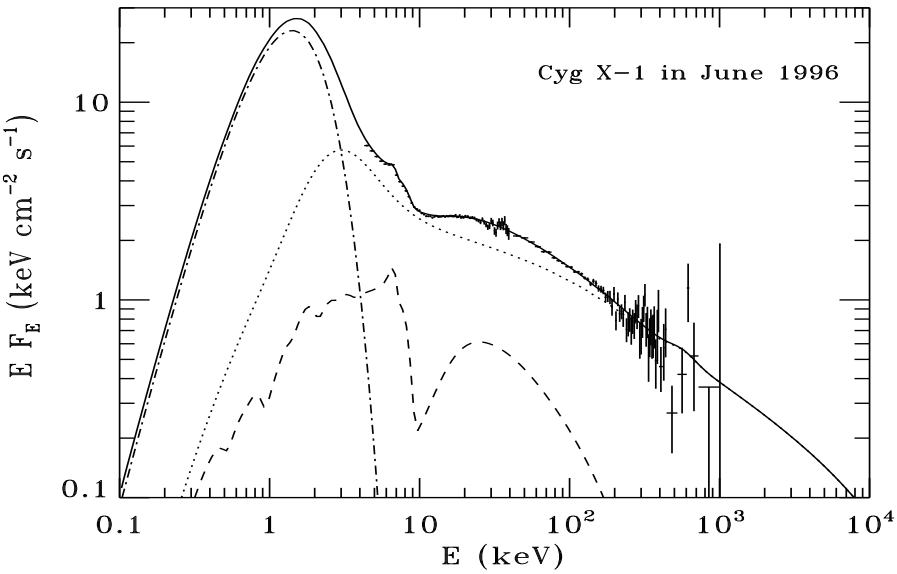

FIGURE 7. The soft state of Cygnus X-1 observed by *RXTE* and OSSE in June 1996 and the best fit hybrid thermal/non-thermal pair model (corrected for interstellar absorption). The solid curve represents the total spectrum, the dashed curve gives the Compton reflection spectrum, and the dotted curve represents the Comptonized continuum. The disc blackbody is shown by the dot-dashed curve. The parameters of the fit are: $l_s = 20$ (frozen), $l_h/l_s = 0.3$, $l_{nth}/l_h = 0.95$, $\tau_p = 0.3$, $kT_{\rm bb} = 0.36$ keV, $\Gamma_{inj} = 3.0$, $R = 0.4$, $\xi = 3.7 \cdot 10^3$, giving a χ^2/dof=168/167. The temperature of the Maxwellian part of the electron distribution is $kT_e = 30$ keV, and the total Thomson optical depth (including pairs) $\tau_T = 0.32$. The iron edge and the iron line appear to be smeared (requiring to account for rotation of the relativistic accretion disc, see Życki *et al.* 1997a,b; Gierliński *et al.* 1997b) and the reflector to be ionised.

May 30, 1996, while Cui *et al.* (1997) get $R \approx 0.15$ (restricting themselves to a much narrower energy range). Both, the iron line and the iron edge, appear to be smeared due to probably gravitational redshift and Doppler effect, implying that the cold disc extends very close to the central black hole.

The origin of the steep power-law was interpreted in terms of bulk Comptonization in a converging flow (Ebisawa, Titarchuk, & Chakrabarti 1996; Titarchuk, Mastichiadis, & Kylafis 1997). This model predicts a cutoff at $\lesssim m_e c^2$ which does not appear to be the case. The power-law can be produced by Comptonization of soft photons from the accretion disc by a non-thermal corona (the base of the jet?) which is optically thin and covers much of that disc (Mineshige, Kusunose & Matsumoto 1995; Li *et al.* 1996a,b; Li & Miller 1997; Liang & Narayan 1997; Poutanen & Coppi 1998). In that case, the turnover is expected at a few MeV due to absorption by photon-photon pair production.

3.2.2. *Hybrid pair plasma model*

The steep power-law in the γ-ray spectral region can be interpreted as a Comptonization (or, in fact, a single scattering) by *non-thermal* electrons ($e^{\pm}$ pairs), and an additional component peaking at ~ 3 keV as a *thermal* Comptonization by rather low temperature electrons. It is natural to assume that both components are produced in the same spatial region by electrons having a non-Maxwellian distribution.

The soft state data are shown on Figure 7 together with the model spectrum. Unfortunately, data in the γ-rays are not good enough to determine the compactnesses

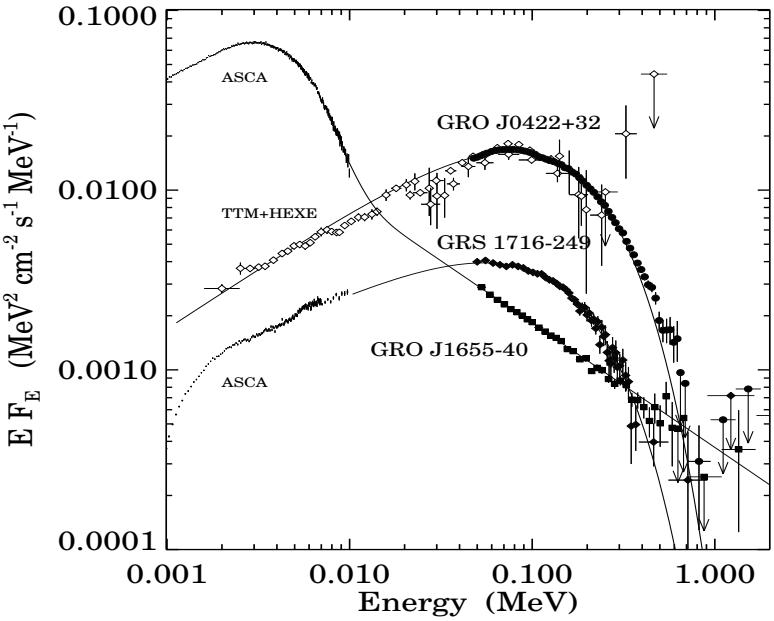

FIGURE 8. Different spectral classes of Galactic black holes (from Grove *et al.* 1998).

unambiguously (one needs very accurate estimates of the amplitude of the annihilation line, as well as shape of the cutoff at $\sim 5-10$ MeV). It is worth mentioning once more that the whole spectrum from soft X-rays to γ-rays can be represented by a hybrid model where the electron distribution is determined self-consistently by balancing heating, acceleration and cooling.

3.3. *Spectral state transitions*

Some Galactic black holes have been observed to always be in one of the states (either in the hard, or in the soft), while others have shown transitions between states (see Fig. 8, and Sunyaev *et al.* 1991; Grove *et al.* 1997b; Grebenev *et al.* 1997). The nature of the state transitions is not fully understood yet, and none of the dynamical accretion disc models can fully describe them. Probably, the most developed model presently available is the advection dominated accretion disc model (see Esin *et al.* 1997, 1998, and article by R. Narayan *et al.* in this volume). This model is able to explain general spectral behaviour in the X-ray range, during the transition. However, restricted to pure thermal plasma, it is not able to explain the γ-ray data.

We restrict our consideration here to the observations and spectral modelling of Cyg X-1. During the transition from the hard to the soft state, the γ-ray luminosity drops, the spectrum becomes steeper, while the cutoff energy increases (Phlips *et al.* 1996; Poutanen 1998). The luminosities of the different spectral components change dramatically in expense of each other, while the bolometric luminosity hardly changes (Zhang *et al.* 1997).

In the hard state, most of the power is deposited, through the thermal channel, to heat the plasma of the inner accretion disc. The non-thermal supply is relatively small, resulting in a weak observed tail at MeV energies. The soft photon input to the system

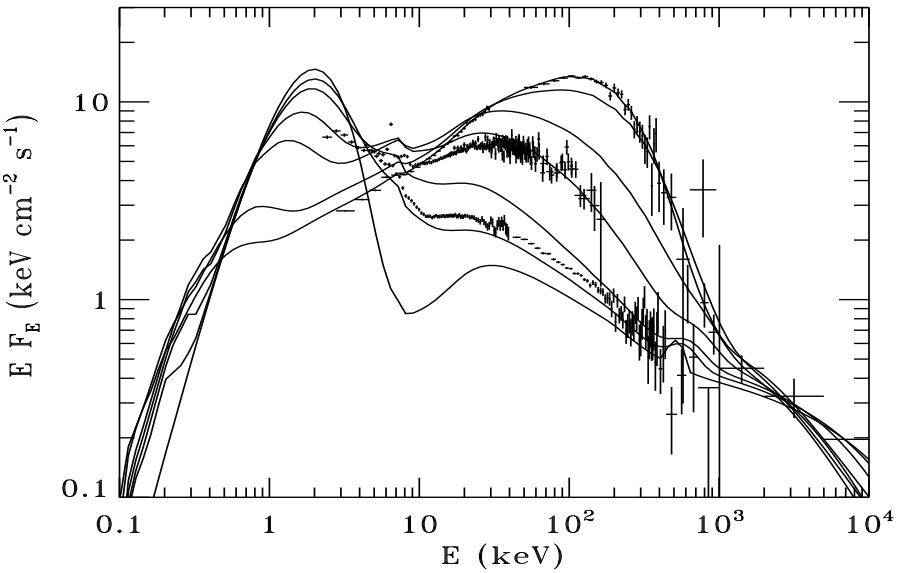

FIGURE 9. Spectral states of Cyg X-1 and the state transition as predicted by the hybrid pair model.

is also rather small. Thus the system is "photon starved" and produces a hard spectrum. Soft photons that are Comptonized to X/γ-rays by thermal electrons are most probably produced by reprocessing of the X/γ-rays in the cold material. This feedback effect fixes the spectral index at a value that is defined by the geometry of the system.

In the soft state, the soft photon luminosity (from the accretion disc) exceeds all other energy injection rates to the system, while thermal energy dissipation (electron heating in the corona/hot disc) is negligible. The non-thermal energy injection rate is $\sim 1/4$ of the total energy output of the system. This almost pure non-thermal model reproduces the broad-band soft state data (see Fig. 7 and Gierliński *et al.* 1998).

Poutanen & Coppi (1998) showed that by using simple scaling laws for the luminosity of the cold disc, the thermal dissipation/heating rate in the corona, and the rate of energy injection from a non-thermal source, all as functions of radius of the corona, the hard-to-soft transition can be explained as the result of a decrease in the transition radius between the inner hot disc (corona) and the outer cold disc by a factor ~ 5. They assumed that the sum of the soft luminosity from the disc, $L_s \propto 1/r$, and the thermal dissipation rate in the corona, $L_{th} \propto 1 - 1/r$, as well as the non-thermal power, L_{nth}, remain approximately constant during transition. This idea is somewhat similar to the proposal by Mineshige *et al.* (1995) (although they fixed the ratio l_{nth}/l_{th}). The model gives a sequence of spectra, shown in Figure 9 together with the data of Cyg X-1. When transition radius decreases, the ratio l_h/l_s (and the spectral index) does not change until the internally generated soft photon luminosity becomes comparable to the reprocessed one. After that the spectrum changes dramatically since l_h/l_s decreases. The model explains the pivoting behaviour of the spectra at ~ 10 keV, and predicts a pivoting behaviour at $\gtrsim 1$ MeV. Smaller soft γ-ray luminosity in the soft state results in a decrease of the pair production opacity, giving a higher cutoff energy. The predicted behaviour in the MeV range can be compared with observations only after the launch of INTEGRAL.

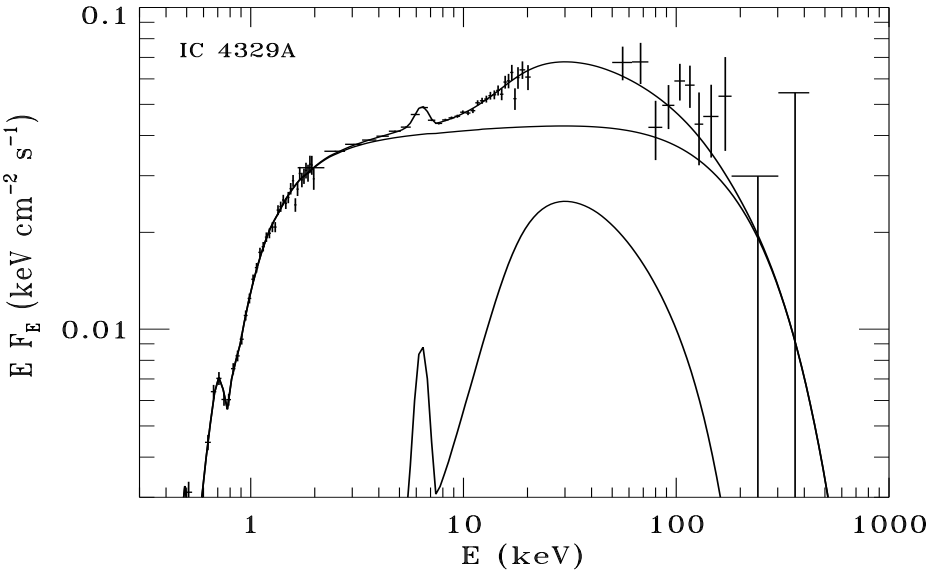

FIGURE 10. The ROSAT/*Ginga*/OSSE broad-band spectrum of Seyfert 1 galaxy, IC4329A (data from Madejski *et al.* 1995). The dashed line is the thermal Comptonization spectrum from a spherical cloud of electron temperature $kT_e = 85$ keV and radial optical depth $\tau = 1.1$. The temperature of the soft seed photons, $kT_{\rm bb}$, is fixed at 35 eV. Calculation are made for the geometry of the X/γ-ray source where cold accretion disc is situated outside of a hot central spherical cloud (see Poutanen *et al.* 1997; Dove *et al.* 1997). The amount of Compton reflection is factor of 3 larger than expected from an infinite geometrically thin cold slab.

4. Seyfert galaxies

Broad-band spectral properties of Seyfert (Sy) galaxies are discussed in recent reviews by Zdziarski *et al.* (1997), Johnson *et al.* (1997) (see also a review by G. Madejski in this volume).

4.1. *"Normal" Seyfert 1 galaxies*

4.1.1. *Observations*

X-ray/gamma-ray spectra of Sy 1s are very similar to the hard state of GBHs (see Fig. 10), having a power-law spectral index $\alpha \approx 1$ and cutoff energies $E_c \approx 300$ keV (e.g., Gondek *et al.* 1996). The spectral hardening at ~ 10 keV is also detected in Seyferts (Nandra & Pounds 1994; Weaver, Arnaud & Mushotzky 1995). An important difference is that the amount of Compton reflection is generally found to be somewhat higher, $R \sim 0.8$ (Gondek *et al.* 1996; Zdziarski *et al.* 1997). Probably, the only exception is NGC 4151 which has almost an identical spectrum to the one of the GBHs GX 339-4 (Zdziarski *et al.* 1998), and $R \approx 0.4$ (Zdziarski, Johnson & Magdziarz 1996). Radio quiet Sy have not been detected in the γ-ray spectral range (Maisack *et al.* 1995). Spectral similarities with GBHs support the attribution of the X/γ spectra to a scale invariant process, such as Compton scattering. Best fits with thermal Comptonization models to the broad-band data give $kT_e \approx 100$ keV and $\tau_T \approx 1$.

4.1.2. *Geometry*

The *slab-corona* model (Liang 1979; Haardt & Maraschi 1991, 1993) predict slopes of the Comptonized spectrum $\alpha \sim 1$, if all the energy is dissipated in the corona. Harder

X-ray spectra can be achieved only if the coronal temperature is high enough ($\gtrsim 300$ keV) to make an anisotropy break in the observed band (Stern *et al.* 1995b; Svensson 1996a,b). Let us consider as an example one of the brightest Sy 1s, IC 4329A. Spectral fitting to the broad-band data (Madejski *et al.* 1995) gives $kT_e = 80$ keV and $\tau_T = 0.7$ (assuming $kT_{\rm bb} = 35$ eV). However, this model can be ruled out by the requirement of energy balance. For a given τ_T, the reprocessed flux from the cold slab would cool down the corona to 45 keV. Internal dissipation in the cold slab would worsen the discrepancy. Similar conclusion can be drawn for the averaged spectrum of Sy 1s (Zdziarski *et al.* 1997).

Flares. Since in Seyferts, the amplitude of Compton reflection, R, is closer to 1 than in GBHs, one could argue that active region (magnetic flares) model is more viable here. Indeed, having less soft photon returning to the active region, the spectra (harder than in the slab-corona case) satisfy the energy balance condition, and produce the needed amount of Compton reflection. The anisotropy break (never seen in Seyferts) shifts to smaller energies, out of the observed X-ray band, due to smaller (than in GBHs) characteristic energies of soft seed photons.

Cloudlets. The hardness of the spectrum of IC 4329A, provides limits on the covering factor of the cold clouds. The energy balance can be satisfied for $f_c \lesssim 1/3$ (similar to GX 339-4, see Fig. 2; note that curves corresponding to a constant l_h/l_s for $kT_{\rm bb} = 35$ eV are shifted a little to the left). Larger f_c would cool down the hot slab by the reprocessed radiation. For $f_c = 1/3$ (no energy dissipation in clouds is allowed), the best fit to the data gives $kT_e = 70$ keV and the optical thickness of the half-slab $\tau_T = 0.6$. This model requires Compton reflection to be produced externally.

Sombrero. Models with a hot inner disc (modelled as a sphere) and a cold outer disc, give acceptable fits. They are energetically possible if $r_{in}/r_c \gtrsim 0.7$. For $r_{in}/r_c = 0.7$ the best fit gives $kT_e = 75$ keV and $\tau_T = 1.5$, and for $r_{in}/r_c = 1$, $kT_e = 85$ keV and $\tau_T = 1.1$ (see Fig. 10). Both, the sombrero model (where the cold disc is modelled as an infinite, geometrically thin, slab) and the cloudlets model predict too little Compton reflection. Probably, it can be provided by a material far away from the center and plane of the disc (molecular torus, see Krolik *et al.* 1994; Ghisellini *et al.* 1994). This can be checked by the response of the reflection component on changes in the amplitude of the continuum.

4.2. *Seyfert 2s*

Seyfert 2 galaxies have generally higher column densities of the absorber towards the nuclei, than Sy 1s do, so that their intrinsic (nuclear) radiation is not always directly observable (see, e.g. Smith, Done & Pounds 1993; Done, Madejski & Smith 1996; Matt *et al.* 1997). On the other hand, hard X-ray/soft γ-ray spectra of Sy 2s and Sy 1s are very similar (Zdziarski *et al.* 1997; Johnson *et al.* 1997) as predicted by the unification schemes of Seyfert galaxies (Antonucci 1993), and there are no really strong arguments that the intrinsic spectra of Sy 2s are somewhat different from that of Sy 1s.

4.3. *Narrow line Seyfert 1 galaxies*

Another class of Seyfert galaxies, the ultra soft narrow-line Seyfert 1 galaxies (NLSy 1), is characterized by a large soft X-ray excess (very steep spectrum in the soft X-rays) and somewhat steeper (softer) spectra in the standard (1-10 keV) X-ray range (see Turner *et al.* 1993; Pounds, Done & Osborne 1995, Brandt, Mathur & Elvis 1997). Their hard X-ray properties are unknown. Pounds *et al.* (1995) interpreted these objects as Seyferts in their soft (high) state. One would think that in that case, broad fluorescent iron lines should appear in these objects more often than in "normal" Seyferts, since the inner edge of the cold disc should be closer to the central black hole in order to produce large

soft X-ray luminosity. One can expect some indications of the correlations between the spectral index and the width of the iron line. We certainly need better data to make further progress in understanding these objects.

5. Final remarks

One of the most intriguing developments during recent years, is the understanding that X/γ-ray spectra of stellar mass black holes (in their hard states) are very similar to the spectra of active galactic nuclei, that are believed to contain $10^6 - 10^8$ solar masses. The spectral fits to the data with the thermal Comptonization models give values of the electron temperature within 50–100 keV and a Thomson optical depth (of the slab) close to unity. These observations give more support to the scale free accretion disc models of the central engine and to Comptonization as the most important scale free radiative process. There are, however, a few questions that have to be addressed.

What is the physical reason for τ_T to be ~ 1? If the plasma is $e^{\pm}$ pair dominated, $\tau_T \sim 1$ is a natural limit just because it is difficult to get compactnesses larger than $\sim 10^3$. Such a compactness is at least an order of magnitude above the estimate, given by the known X/γ-ray luminosity and sizes inferred from the inner edge of the outer cold disc. Significant contribution from non-thermal processes and inhomogeneous energy dissipation probably can remove this discrepancy. On the other hand, $\tau_T \sim 1$ can be achieved in the hot accretion discs radiating at the maximum accretion rate limited by advection (Zdziarski 1998).

What is the geometry of the X/γ-ray producing region in GBHs and Seyferts? Magnetic flares above a cold accretion disc are still a possible solution for Seyferts. We argued that in the case of GBHs, a hot inner disc with a cold disc outside is a more plausible geometry. This can also be a *unifying geometry for both GBHs and Seyferts*. Larger amplitude of the Compton reflection observed in Seyferts can be due to the contribution from the molecular torus. On the other hand, the presence of the gravitationally redshifted fluorescent iron lines in the spectra of some Seyferts (implying inner radius of the cold disc to be at a few GM/c^2, see, e.g., Tanaka *et al.* 1995; Fabian *et al.*; Nandra *et al.* 1997) would be more difficult to explain in such a geometry.

An important observational progress, made during recent years, was the broad-band X/γ-ray data of GBHs in their soft state. Luckily for us, the soft state transition was observed in Cyg X-1 in the summer of 1996. These observations revealed that the soft state spectra cannot be explained by thermal Comptonization. Hybrid thermal/non-thermal model gives an acceptable description of the broad-band data (from soft X-ray to MeV), making predictions for the spectral change in the MeV range. Unfortunately, we will have to wait for INTEGRAL, before we can verify these predictions. This model also successfully reproduces spectral transitions, as a results of redistribution of the energy dissipation between the hot inner cloud and the cold outer disc, with a constant non-thermal energy injection, probably by the base of the jet or non-thermal corona. Thus, the hybrid model can be a *unifying link between hard and soft states of GBHs*. What is the physical reason for the change in the transition radius between hot and cold phases? We do not know the answer yet.

In the soft state, the inner radius of the cold disc moves closer to the central black hole. The profile of the iron line should change notably and smearing of the iron edge is expected due to the Doppler effect and gravitational redshift. Simultaneous data with a high spectral resolution and a broad spectral coverage (to determine continuum unambiguously) are required to quantify the amplitude of these effects. Observationally

it is a challenge, since the soft blackbody bump (in GBHs) dominates in the spectral region around the iron line.

In the case of Seyferts, it is possible that those objects that show redshifted iron lines belong to the NLSy 1 class (probably, the "soft state" Seyferts, see, e.g., Lee *et al.* 1998 for the case of MCG-6-30-15). Then, the correlation between the spectral index and the width of the iron line is expected. We can speculate that NLSy 1 are analogous to the soft state GBHs, but observationally this is not well established yet.

This research was supported by grants from the Swedish Natural Science Research Council and from the Anna-Greta and Holger Crafoord's Fund. The author thanks A. Zdziarski, M. Gierliński, R. Svensson, E. Grove, and F. Haardt for various help during preparation of this review. I also would like to thank the organizers of the Symposium on Non-Linear Phenomena in Accretion Discs around Black Holes for the financial support.

REFERENCES

Antonucci, R. 1993 Unified models for active galactic nuclei and quasars. *Ann. Rev. Astr. Astroph.* **31**, 473–521.

Bałucińska, M. & Hasinger, G. 1991 EXOSAT observations of Cygnus X-1: study of the soft X-ray excess. *Astronomy and Astrophysics* **241**, 439–450.

Bałucińska-Church, M., Belloni, T., Church, M. J. & Hasinger, G. 1995 Identification of the soft X-ray excess in Cygnus X-1 with disc emission. *Astronomy and Astrophysics* **302**, L5–L8.

Bisnovatyi-Kogan, G. S. & Blinnikov, S. I. 1977 Disk accretion onto a black hole at subcritical luminosity. *Astronomy and Astrophysics* **59**, 111–125.

Brandt, W. N., Mathur, S. & Elvis, M. 1997 A comparison of the hard ASCA spectral slopes of broad- and narrow-line Seyfert 1 galaxies. *Monthly Not. Roy. Astron. Soc.* **285**, L25–L28.

Celotti, A., Fabian, A. C. & Rees, M. J. 1992 Dense thin clouds in the central regions of active galactic nuclei. *Monthly Not. Roy. Astron. Soc.* **255**, 419–422.

Collin-Souffrin, S., Czerny, B., Dumont, A.-M. & Życki, P. T. 1996 Quasi-spherical accretion of optically thin clouds as a model for the optical/UV/X-ray emission of AGN. *Astronomy and Astrophysics* **314**, 393–413.

Coppi, P. S. 1992 Time-dependent models of magnetized pair plasmas. *The Astrophysical Journal* **258**, 657–683

Coppi, P. S., Zdziarski, A. A. & Madejski, G. M. 1998 EQPAIR: hybrid thermal/nonthermal model for compact sources. *Monthly Not. Roy. Astron. Soc.* , in preparation.

Cui, W., Ebisawa, K., Dotani, T. & Kubota, A. 1997 Simultaneous ASCA and RXTE observations of Cygnus X-1 during its 1996 state transition. *The Astrophysical Journal* **493**, L75–L78.

Cui, W. *et al.* 1997 Rossi X-ray timing explorer observation of Cygnus X-1 in its high state. *The Astrophysical Journal* **474**, L57–L60.

Dermer, C. D. & Liang, E. P. 1989 Electron thermalization and heating in relativistic plasmas. *The Astrophysical Journal* **339**, 512–528.

Dermer, C. D., Miller, J. A. & Li, H. 1996 Stochastic particle acceleration near accreting black holes. *The Astrophysical Journal* **456**, 106–118.

Done, C., Madejski, G. M. & Smith, D. A. 1996 NGC 4945: the brightest Seyfert 2 galaxy at 100 keV. *The Astrophysical Journal* **463**, L63–L66.

Done, C., Mulchaey, J. S., Mushotzky, R. F. & Arnaud, K. A. 1992 An ionized accretion disk in Cygnus X-1. *The Astrophysical Journal* **395**, 275–288.

Dove, J. B., Wilms, J., Maisack, M. & Begelman M. C. 1997 Self-consistent thermal

accretion disk corona models for compact objects. II. Application to Cygnus X-1. *The Astrophysical Journal* **487**, 759–768.

Ebisawa, K., Titarchuk, L. & Chakrabarti, S. K. 1996 On the spectral slopes of the hard X-ray emission from black hole candidates. *Publ. Astron. Soc. Japan* **48**, 59–65.

Ebisawa, K., Ueda, Y., Inoue, H., Tanaka, Y. & White, N. E. 1996 *ASCA* observations of the iron line structure in Cygnus X-1. *The Astrophysical Journal* **467**, 419–434.

Esin, A. A., McClintock, J. E. & Narayan, R. 1997 Advection-dominated accretion and the spectral states of black hole X-ray binaries: application to Nova Muscae 1991. *The Astrophysical Journal* **489**, 865–889.

Esin, A. A., Narayan, R., Cui, W., Grove, E. C. & Zhang, S.-N. 1998 Spectral transitions in Cyg X-1 and other black hole X-ray binaries. *The Astrophysical Journal* submitted (astro-ph/9711167).

Fabian, A. C., Blandford, R. D., Guilbert, P. W., Phinney, E. S. & Cuellar, L. 1986 Pair-induced spectral changes and variability in compact X-ray sources. *Monthly Not. Roy. Astron. Soc.* **221**, 931–945.

Fabian, A. C. *et al.* 1995 On broad iron Kα lines in Seyfert 1 galaxies. *Monthly Not. Roy. Astron. Soc.* **277**, L11–L15.

Galeev, A. A., Rosner, R. & Vaiana, G. S. 1979 Structured coronae of accretion disks. *The Astrophysical Journal* **229**, 318–326.

George, I. M. & Fabian A. C. 1991 X-ray reflection from cold matter in active galactic nuclei and X-ray binaries *Monthly Not. Roy. Astron. Soc.* **249**, 352–367.

Ghisellini, G. & Haardt, F. 1994 On thermal Comptonization in $e^{\pm}$ pair plasmas. *The Astrophysical Journal* **429**, L53–L56.

Ghisellini, G. & Svensson, R. 1990 Synchrotron self-absorption as a thermalizing mechanism. In *Physical Processes in Hot Cosmic Plasmas* (ed. W. Brinkmann, A. C. Fabian & F. Giovannelli) pp. 395–400. Kluwer.

Ghisellini, G., Haardt, F. & Fabian, A. C. 1993 On re-acceleration, pairs and the high-energy spectrum of AGN and Galactic black hole candidates. *Monthly Not. Roy. Astron. Soc.* **263**, L9–L12.

Ghisellini, G., Haardt, F. & Matt, G. 1994 The contribution of the obscuring torus to the X-ray spectrum of Seyfert galaxies: a test for the unification model. *Monthly Not. Roy. Astron. Soc.* **267**, 743–754.

Ghisellini, G., Haardt, F. & Svensson 1998 Thermalization by synchrotron absorption in compact sources: electron and photon distribution. *Monthly Not. Roy. Astron. Soc.* in press (astro-ph/9712166).

Gierliński, M. *et al.* 1997a Simultaneous X-ray and gamma-ray observations of Cyg X-1 in the hard state by Ginga and OSSE. *Monthly Not. Roy. Astron. Soc.* **288**, 958–964.

Gierliński, M., Zdziarski, A. A., Dotani, T., Ebisawa, K., Jahoda, K. & Johnson, W. N. 1997b X-ray and gamma-ray spectra of Cyg X-1 in the soft state. In *Proceedings of 4th Compton Symposium* (ed. C. D. Dermer, M. S. Strickman, & J. D. Kurfess). AIP Conference Proceedings, vol. 410, pp. 844–848. AIP.

Gierliński, M., Zdziarski, A. A., Coppi, P. S., Poutanen, J., Ebisawa, K. & Johnson, W. N. 1998 Thermal/non-thermal model of Cyg X-1 in the soft state In *Proceedings of the Symposium The Active X-ray Sky* (ed. L. Scarsi, H. Brandt, P. Giommi, & F. Fiore). *Nuclear Physics B Proceedings Suppl.* in press.

Gondek, D. *et al.* 1996 The average X-ray/gamma-ray spectrum of radio-quite Seyfert 1s *Monthly Not. Roy. Astron. Soc.* **282**, 646–652.

Grebenev, S. A. *et al.* 1993 Observations of black hole candidates with GRANAT. *The Astrophysical Journal Suppl.* **97**, 281–287.

Grebenev, S. A., Sunyaev, R. A., & Pavlinsky, M. N. 1997 Spectral states of galactic black hole candidates: results of observations with ART-P/Granat. *Adv. Space Res.* **19**, (1)15–(1)23.

Grove, J. E., Grindlay, J. E., Harmon, B. A., Hua, X.-M., Kazanas, D. & McConnell,

M. 1997a Galactic black hole binaries: high energy radiation. In *Proceedings of 4th Compton Symposium* (ed. C. D. Dermer, M. S. Strickman, & J. D. Kurfess). AIP Conference Proceedings, vol. 410, pp. 122–140. AIP.

Grove, J. E., Kroeger, R. A. and Strickman, M. S. 1997b Two gamma-ray spectral classes of black hole transients. In *The Transparent Universe.* (ed. C. Winkler, T. J.-L. Courvoisier, & Ph. Durouchoux) Proceedings 2nd INTEGRAL Workshop, SP-382, pp. 197–200. ESA.

Grove, J. E. *et al.* 1998 Gamma-ray spectral states of Galactic black hole candidates. *The Astrophysical Journal* **499**, in press.

Haardt, F. 1997 Models for the X-ray emission from radio quiet AGNs. *Mem. Soc. Astron. Ital.* **68**, 73–80. (astro-ph/9612082).

Haardt, F. & Maraschi, L. 1991 A two-phase model for the X-ray emission from Seyfert galaxies. *The Astrophysical Journal* **380**, L51–L54.

Haardt, F. & Maraschi, L. 1993 X-ray spectra from two-phase accretion disks. *The Astrophysical Journal* **413**, 507–517.

Haardt, F., Maraschi, L. & Ghisellini, G. 1994 A model for the X-ray and UV emission from Seyfert galaxies and galactic black holes. *The Astrophysical Journal* **432**, L95–L99.

Johnson, W. N., Zdziarski, A. A., Madejski, G. M., Paciesas, W. S., Steinle, H. & Lin, Y.-C. 1997 Seyferts and radio galaxies. In *Proceedings of 4th Compton Symposium* (ed. C. D. Dermer, M. S. Strickman, & J. D. Kurfess). AIP Conference Proceedings, vol. 410, pp. 283–305. AIP.

Krolik, J. H., Madau, P. & Życki, P. T. 1994 X-ray bumps, iron Kα lines, and X-ray suppression by obscuring tori in Seyfert galaxies. *The Astrophysical Journal* **420**, L57–L61.

Kuncic, Z., Celotti, A., & Rees, M. J. 1997 Dense, thin clouds and reprocessed radiation in the central regions of of active galactic nuclei. *Monthly Not. Roy. Astron. Soc.* **284**, 717–730.

Lee, J. C., Fabian, A. C., Reynolds, C. S., Iwasawa, K. & Brandt, W. N. 1998 An RXTE observation of the Seyfert 1 galaxy MCG-6-30-15: X-ray reflection and the iron abundance. *Monthly Not. Roy. Astron. Soc.* submitted.

Li, H., Kusunose, M. & Liang, E. P. 1996a Gamma rays from Galactic black hole candidates with stochastic particle acceleration. *The Astrophysical Journal* **460**, L29–L32.

Li, H., Kusunose, M. & Liang, E. P. 1996b Non-thermal high energy emission and stochastic particle acceleration in galactic black holes. *Astronomy and Astrophysics Suppl.* **120C**, 167–170.

Li, H. & Miller, J. A. 1997 Electron acceleration and the production of nonthermal electron distributions in accretion disk coronae. *The Astrophysical Journal* **478**, L67–L70.

Liang, E. P. T. 1979 On the hard X-ray emission mechanism of active galactic nuclei sources. *The Astrophysical Journal* **231**, L111–L114.

Liang, E. P. 1991 Structure of thermal pair clouds around gamma-ray–emitting black holes. *The Astrophysical Journal* **367**, 470–475.

Liang, E. P. & Dermer, C. D. 1988 Interpretation of the gamma-ray bump from Cygnus X-1 *The Astrophysical Journal* **325**, L39–L42.

Liang, E. P. & Narayan, R. 1997 Spectral signatures and physics of black hole accretion disks. In *Proceedings of 4th Compton Symposium* (ed. C. D. Dermer, M. S. Strickman, & J. D. Kurfess). AIP Conference Proceedings, vol. 410, pp. 461–476. AIP.

Lightman, A. P. 1974 Time-dependent accretion disks around compact objects. II. Numerical models and instability of inner region. *The Astrophysical Journal* **194**, 429–437.

Lightman, A. P. & Zdziarski, A. A. 1987 Pair production and Compton scattering in compact sources and comparison to observations of active galactic nuclei. *The Astrophysical Journal* **319**, 643–661.

Ling, J. C. *et al.* 1997 Gamma-ray spectra and variability of Cygnus X-1 observed by BATSE. *The Astrophysical Journal* **484**, 375–382

Maciołek-Niedźwiecki, A., Zdziarski, A. A. & Coppi, P. S. 1995 Electron-positron pair production and annihilation spectral features from compact sources. *Monthly Not. Roy.*

Astron. Soc. **276**, 273–292.

Madejski, G. M. *et al.* 1995 Joint *ROSAT-COMPTON GRO* observations of the X-ray-bright Seyfert galaxy IC 4329A. *The Astrophysical Journal* **438**, 672–679.

Magdziarz, P. & Zdziarski, A. A. 1995 Angle-dependent Compton reflection of X-rays and gamma-rays. *Monthly Not. Roy. Astron. Soc.* **273**, 837–848.

Maisack, M. *et al.* 1995 Upper limits on the MeV emission of Seyfert galaxies. *Astronomy and Astrophysics* **298**, 400–404.

Matt, G. *et al.* 1997 Hard X-ray detection of NGC 1068 with BeppoSAX. *Astronomy and Astrophysics* **325**, L13–L16.

McConnell, M. L. *et al.* 1994 Observations of Cygnus X-1 by COMPTEL during 1991. *The Astrophysical Journal* **424**, 933–939.

Mineshige, S., Kusunose, M. & Matsumoto, R. 1995 Low-state disks and low-beta disks. *The Astrophysical Journal* **445**, L43–L46.

Nagirner, D. I. & Poutanen, J. 1994 Single Compton scattering. *Astrophys. Space Phys. Reviews* **9**, 1–83.

Nandra, K. & Pounds, K. A. 1994 *Ginga* observations of the X-ray spectra of Seyfert galaxies. *Monthly Not. Roy. Astron. Soc.* **268**, 405–429.

Nandra, K. *et al.* 1997 *ASCA* observations of Seyfert 1 galaxies. II. Relativistic iron Kα emission. *The Astrophysical Journal* **477**, 602–622.

Nayakshin, S. & Melia, F. 1998 Self-consistent Fokker-Planck treatment of particle distributions in astrophysical plasmas. *The Astrophysical Journal Suppl.* **114**, 269–288.

Phlips, B. F. *et al.* 1996 Gamma-ray observations of Cygnus X-1 with oriented scintillation spectrometer experiment. *The Astrophysical Journal* **465**, 907–914.

Pietrini, P. & Krolik, J. H. 1995 The inverse Compton thermostat in hot plasmas near accreting black holes. *The Astrophysical Journal* **447**, 526–544.

Pilla, R. P. & Shaham, J. 1997 Kinetic of electron-positron pair plasmas using an adaptive Monte-Carlo method. *The Astrophysical Journal* **486**, 903–918.

Pounds, K. A., Done, C. & Osborne, J. P. 1995 RE 1034+39: a high-state Seyfert galaxy? *Monthly Not. Roy. Astron. Soc.* **277**, L5–L10.

Poutanen, J. 1998 Modeling X/γ-ray spectra of Galactic black holes and Seyferts. In *Accretion Processes in Astrophysical Systems: Some Like It Hot* (ed. S. S. Holt & T. Kallman). AIP Conference Proceedings, in press. AIP. (astro-ph/9801055).

Poutanen, J. & Coppi, P. S. 1998 Unification of spectral states of accreting black holes. *Physica Scripta* in press (astro-ph/9711316).

Poutanen, J. & Svensson, R. 1996 The two-phase pair corona model for active galactic nuclei and X-ray binaries: How to obtain exact solutions. *The Astrophysical Journal* **470**, 249–268

Poutanen, J., Krolik, J. H. & Ryde, F. 1997 The nature of spectral transitions in accreting black holes: the case of Cyg X-1. *Monthly Not. Roy. Astron. Soc.* **292**, L21–L25.

Poutanen, J., Nagendra, K. N. & Svensson, R. 1996 Green's matrix for Compton reflection of polarized radiation from cold matter. *Monthly Not. Roy. Astron. Soc.* **283**, 892–904

Pozdnyakov, L. A., Sobol, I. M. & Sunyaev, R. A. 1983 Comptonization and the shaping of X-ray source spectra – Monte-Carlo calculations. *Sov. Sci. Rev. E Astrophys. Space Phys.* **2**, 189–331.

Rybicki, G. B. & Lightman, A. P. 1979 Radiative Processes in Astrophysics. Wiley.

Smith, D. A., Done, C. & Pounds, K. A. 1993 Unified theories of active galactic nuclei: the hard X-ray spectrum of NGC 1068. *Monthly Not. Roy. Astron. Soc.* **263**, 54–60.

Stern, B. E. 1985 On the possibility of efficient production of electron-positron pairs near pulsars and accreting black holes. *Sov.Astr.* **29**, 306–313.

Stern, B. E. 1988 Nonthermal pair production in active galactic nuclei: A detailed radiation transfer model. *Nordita/88-51 A*, preprint.

Stern, B. E., Begelman, M. C., Sikora, M. & Svensson, R. 1995a A large-particle Monte Carlo code for simulating non-linear high-energy processes near compact objects. *Monthly*

Not. Roy. Astron. Soc. **272**, 291–307.

Stern, B. E., Poutanen, J., Svensson, R., Sikora, M. & Begelman M. C. 1995b On the geometry of the X-ray emitting region in Seyfert galaxies. *The Astrophysical Journal* **449**, L13–L17.

Shapiro, S. L., Lightman, A. P. & Eardley D. N. 1976 A two-temperature accretion disk model for Cygnus X-1: structure and spectrum. *The Astrophysical Journal* **204**, 187–199.

Sunyaev, R. A. & Titarchuk, L. G. 1980 Comptonization of X-rays in plasma clouds. Typical radiation spectra. *Astronomy and Astrophysics* **86**, 121–138.

Sunyaev, R. A. *et al.* 1991 Three spectral states of 1E 1740.7-2942: from standard Cygnus X-1 type spectrum to the evidence of the electron-positron annihilation feature. *The Astrophysical Journal* **383**, L49–L52.

Svensson, R. 1987 Non-thermal pair production in compact X-ray sources: first order Compton cascades in soft radiation field. *Monthly Not. Roy. Astron. Soc.* **227**, 403–451.

Svensson, R. 1994 The nonthermal pair model for the X-ray and gamma-ray spectra from active galactic nuclei. *The Astrophysical Journal Suppl.* **92**, 585–592.

Svensson, R. 1996a X-rays and Gamma Rays from Active Galactic Nuclei. In *Relativistic Astrophysics: A Conference in Honour of Professor I. D. Novikov's 60th Birthday* (ed. B. J. T. Jones & D. Markovic), pp. 235–249. Cambridge University Press.

Svensson, R. 1996b Models of X-ray and Gamma-Ray Emission from Seyfert Galaxies. *Astronomy and Astrophysics Suppl.* **120C**, 475–480.

Tanaka, Y. 1991 Black hole candidates in binaries. In *Iron line diagnostics in X-ray sources* (ed. A. Treves) Lecture Notes in Physics, vol. 385, pp. 98–110. Springer.

Tanaka, Y. & Lewin, W. H. G. 1995 Black-hole binaries. In *X-ray binaries* (ed. W. H. G. Lewin, J. van Paradijs, E. P. J. van den Heuvel) Cambridge Astrophysics Series, vol. 26, pp. 126–174. Cambridge University Press.

Tanaka, Y. *et al.* 1995 Gravitationally redshifted emission implying an accretion disk and massive black hole in the active galaxy MCG-6-30-15. *Nature* **375**, 659–661.

Titarchuk, L., Mastichiadis, A. & Kylafis, N. D. 1997 X-ray spectral formation in a converging fluid flow: spherical accretion into black holes. *The Astrophysical Journal* **487**, 834–846.

Van der Klis, M. 1995 Rapid aperiodic variability in X-ray binaries. In *X-ray binaries* (ed. W. H. G. Lewin, J. van Paradijs, E. P. J. van den Heuvel) Cambridge Astrophysics Series, vol. 26, pp. 252–307. Cambridge University Press.

Van Dijk, R. *et al.* 1995 The black-hole candidate GRO J0422+32: MeV emission measured with COMPTEL. *Astronomy and Astrophysics* **296**, L33–L36.

Weaver, K. A., Arnaud, K. A. & Mushotzky, R. F. 1995 A confirmation of 2-40 keV spectral complexity in Seyfert galaxies. *The Astrophysical Journal* **447**, 121–138.

White, T. R., Lightman, A. P. & Zdziarski, A. A. 1988 Compton reflection of gamma-rays by cold electrons *The Astrophysical Journal* **331**, 939–948.

Zdziarski, A. A. 1985 Power-law X-ray and gamma-ray emission from relativistic pair plasmas. *The Astrophysical Journal* **289**, 514–525.

Zdziarski, A. A., Ghisellini, G., George, I. M., Svensson, R., Fabian, A. C. & Done, C. 1990 Electron-positron pairs, Compton reflection, and the X-ray spectra of active galactic nuclei. *The Astrophysical Journal* **363**, L1–L4.

Zdziarski, A. A., Gierliński, M., Gondek, D. & Magdziarz, P. 1996a The canonical X-ray/gamma-ray spectrum of Seyfert 1s and low state Galactic black hole candidates. *Astronomy and Astrophysics Suppl.* **120C**, 553–558.

Zdziarski, A. A., Johnson, W. N. & Magdziarz, P. 1996b Broad-band gamma-ray and X-ray spectra of NGC 4151 and their implications for physical processes and geometry. *Monthly Not. Roy. Astron. Soc.* **283**, 193–206.

Zdziarski, A. A., Johnson, W. N., Poutanen, J., Magdziarz, P. & Gierliński, M. 1997 X-rays and gamma-rays from accretion flows onto black holes in Seyferts and X-ray binaries. In *The Transparent Universe.* (ed. C. Winkler, T. J.-L. Courvoisier, & Ph. Durouchoux)

Proceedings 2nd INTEGRAL Workshop, SP-382, pp. 373–380. ESA.

Zdziarski, A. A. 1998 Hot accretion disc with thermal Comptonization and advection. *Monthly Not. Roy. Astron. Soc.* in press.

Zdziarski, A. A., Poutanen, J., Mikołaewska, J., Gierliński, M., Ebisawa, K. & Johnson, W. N. 1998 Simultaneous observations of GX 339-4 by Ginga and OSSE and their astrophysical consequences. *Monthly Not. Roy. Astron. Soc.* submitted.

Zhang S. N., Cui W., Harmon B. A., Paciesas W. S., Remillard R. E. & van Paradijs J. 1997 The 1996 soft state transition of Cygnus X-1. *The Astrophysical Journal* **477**, L95–L98.

Zycki, P. T., Done, C. & Smith, D. A. 1997a Relativistically smeared X-ray reprocessed components in the *Ginga* spectra of GS2023+388. *The Astrophysical Journal* **488**, L113–L116.

Zycki, P. T., Done, C. & Smith, D. A. 1997b Evolution of the accretion flow in Nova Muscae 1991. *The Astrophysical Journal* **496**, L25–L28.